

This discussion paper is/has been under review for the journal *Atmospheric Chemistry and Physics (ACP)*. Please refer to the corresponding final paper in *ACP* if available.

**Characteristics and  
source  
apportionment of  
atmospheric aerosols**

H. Xu et al.

# Characteristics and source apportionment of atmospheric aerosols at the summit of Mount Tai during summertime

H. Xu<sup>1,2</sup>, Y. Wang<sup>1</sup>, T. Wen<sup>1</sup>, Y. Yang<sup>1</sup>, and Y. Zhao<sup>1</sup>

<sup>1</sup>LAPC, Institute of Atmospheric Physics, Chinese Academy of Sciences,  
100029 Beijing, China

<sup>2</sup>Zhejiang Institute of Meteorological Sciences, 310017 Hangzhou, China

Received: 30 June 2009 – Accepted: 24 July 2009 – Published: 31 July 2009

Correspondence to: Y. Wang (wys@dq.cern.ac.cn)

Published by Copernicus Publications on behalf of the European Geosciences Union.

Title Page

Abstract

Introduction

Conclusions

References

Tables

Figures

⏪

⏩

◀

▶

Back

Close

Full Screen / Esc

Printer-friendly Version

Interactive Discussion

## Abstract

To investigate the long-range transport of air pollutants in North China, aerosol samples were collected at the summit of Mount Tai (Shandong province) in June of 2006. Water-soluble ion and metal element concentrations were analyzed using ion chromatography (IC) and inductively coupled plasma-mass spectrometry (ICP-MS), respectively. Results showed three different size distributions for the ions and metal elements characterized, including masses in: (i) the accumulation mode, with a peak at 0.43 to 1.1  $\mu\text{m}$  ( $\text{SO}_4^{2-}$ ,  $\text{NH}_4^+$ ,  $\text{K}^+$ ,  $\text{Pb}$ ,  $\text{Zn}$ ,  $\text{Ti}$ ); (ii) the coarse particle mode, with a peak at 4.7 to 5.8  $\mu\text{m}$  ( $\text{Ca}^{2+}$ ,  $\text{Mg}^{2+}$ ,  $\text{Ca}$ ,  $\text{Mg}$ ,  $\text{Fe}$ ,  $\text{Al}$ ,  $\text{Ba}$ ,  $\text{Mn}$ ); and (iii) a bimodal distribution, with peaks at 0.43 to 0.65  $\mu\text{m}$  and 4.7 to 5.8  $\mu\text{m}$  ( $\text{NO}_3^-$ ,  $\text{Na}^+$ ,  $\text{Cl}^-$ ,  $\text{Na}$ ,  $\text{Co}$ ,  $\text{Ni}$ ,  $\text{Mo}$ ,  $\text{Cu}$ ). When  $\text{SO}_4^{2-}$  was in high concentration, the mass median diameter was between 0.5  $\mu\text{m}$  and 0.8  $\mu\text{m}$ , belonging to the “drop mode”. The concentrations of  $\text{SO}_4^{2-}$ ,  $\text{NO}_3^-$ ,  $\text{NH}_4^+$ , and  $\text{K}^+$  were quite variable. Interestingly,  $\text{SO}_4^{2-}$ ,  $\text{NO}_3^-$ , and  $\text{NH}_4^+$  reached their highest concentrations when the humid air mass was coming from the south. Furthermore, crustal element concentrations increased when the air mass came from the north and pollution element concentrations were elevated when the air mass came from the south.

## 1 Introduction

Atmospheric aerosols consist of complex mixtures of elemental and organic carbon, ammonium, nitrates, sulphates, mineral dust, trace elements, and water. Investigation of the chemical characteristics of these aerosols is important for elucidating particle toxicity and its potential role in climate change (Christoph et al., 2005). Atmospheric aerosol size distributions, along with their chemical compositions, sources, and sinks, are key elements in understanding and managing aerosol health effects (Englert, 2004), visibility, and the climate (Seinfeld and Pandis, 1998). Therefore, it is important to study the chemical characteristics and sources of atmospheric aerosols as well as their spatial and temporal variations.

ACPD

9, 16361–16379, 2009

### Characteristics and source apportionment of atmospheric aerosols

H. Xu et al.

Title Page

Abstract

Introduction

Conclusions

References

Tables

Figures

◀

▶

◀

▶

Back

Close

Full Screen / Esc

Printer-friendly Version

Interactive Discussion

---

**Characteristics and  
source  
apportionment of  
atmospheric aerosols**

---

H. Xu et al.

---

[Title Page](#)[Abstract](#)[Introduction](#)[Conclusions](#)[References](#)[Tables](#)[Figures](#)[⏪](#)[⏩](#)[◀](#)[▶](#)[Back](#)[Close](#)[Full Screen / Esc](#)[Printer-friendly Version](#)[Interactive Discussion](#)

Rapid urbanization and industrial development in China over the past two decades likely led to significant increases in the emission of particles and their gaseous precursors (Streets and Waldhoff, 2000). During June of 2006, we sampled aerosols for a period of one month at the summit of Mount Tai, the highest mountain in the North China Plains. This mountain-top location was selected for its high, location, which enables the sampling of air masses that are more representative of regional characteristics, allows examination of transport paths from other regions in Asia, and it permits the study of exchanges between the planetary boundary layer (PBL) and the free troposphere (Gao et al., 2005). Due to the domination of Pacific high pressure during the summer season, this site also enabled the sampling of air down-wind from a city group center in eastern China. A better understanding of the aerosol characteristics that influence urban atmosphere was thus obtained. Size distributions of water-soluble ions and metal elements in aerosol were also determined in order to distinguish different aerosol sources.

## 2 Experiments and methodologies

### 2.1 Measurement site

The measurement site ( $36^{\circ}16' N$ ,  $117^{\circ}06' E$ ) was in a meteorological observation station located at the summit of Mount Tai (altitude=1534 m a.s.l.), as shown in Fig. 1. This summit overlooks the city of Tai'an, 15 km to the south, which has a population of approximately 500 000. The city of Ji'nan (Shandong province capital) is situated 60 km to the north and has a population of approximately 2.1 million. A few villages are also visible to the north. A famous tourist destination, Mount Tai has a large number of visitors during the summer months (June through September), and several small restaurants and temples are in the area, which also might produce local emissions. Our measurement site, however, was situated in the eastern part of the summit, which is less frequently visited.

---

**Characteristics and  
source  
apportionment of  
atmospheric aerosols**

---

H. Xu et al.

[Title Page](#)[Abstract](#)[Introduction](#)[Conclusions](#)[References](#)[Tables](#)[Figures](#)[⏪](#)[⏩](#)[◀](#)[▶](#)[Back](#)[Close](#)[Full Screen / Esc](#)[Printer-friendly Version](#)[Interactive Discussion](#)

Aerosol samples were collected with an eight-stage low pressure impactor (Andersen Series 20-800, USA) from 1 to 30 June, 2006. Mixed cellulose ester filter substrates (Thermo-Electron Corporation, USA) were employed in all stages, and a flow rate of  $28.3 \text{ L min}^{-1}$  was used. The 50% cut off diameters ( $D_{50}$ ) were 9.0, 5.8, 4.7, 3.3, 2.1, 1.1, 0.65, and  $0.43 \mu\text{m}$ . During the day, aerosol samples collected from 08:00 a.m. to 06:00 p.m. were regarded as “daytime” aerosols, while those collected from 06:30 p.m. to 07:30 a.m. were regarded as “nighttime” aerosols. There was no sampling on the night on 13 June, 2006 and during the day of 27 June because of rainfall and instrument malfunction. A total of 288 aerosol samples were collected. The chemical composition of these samples was analyzed using IC and ICP-MS.

Aerosol samples were also collected at: (i) the subalpine field observation station of the Gongga alpine ecosystem observation and experiment station ( $29^{\circ}35' \text{ N}$ ,  $102^{\circ}00' \text{ E}$ ), (ii) the research station of Changbai Mountain Forest Ecology ( $42^{\circ}24' \text{ N}$ ,  $128^{\circ} \text{ E}$ ), and (iii) the Dinghushan Forest Ecosystem Research Station ( $23^{\circ}10' \text{ N}$ ,  $112^{\circ}32' \text{ E}$ ), as shown in Fig. 1. Samples were gathered using the high volume sampler (ASI/GMW HVPM10, Thermo-Electron corporation, USA) on 7, 14, 21, and 28 June 2006, respectively. Each collection period was 24 h long, and 12  $\text{PM}_{10}$  samples were collected in total. IC analysis was performed on these samples.

## 2.2 Chemical analysis

### 2.2.1 Ion analysis

Half of each sample and a blank were ultrasonically extracted using 50 ml of water (deionized  $\text{H}_2\text{O}$ ;  $18 \text{ M}\Omega \text{ cm}^{-1}$  resistivity). After passing each extracted sample through a microporous membrane (pore size= $0.45 \mu\text{m}$ ; diameter=25 mm; Ampel Co.), three anions ( $\text{SO}_4^{2-}$ ,  $\text{NO}_3^-$ ,  $\text{Cl}^-$ ) and five cations ( $\text{NH}_4^+$ ,  $\text{Ca}^{2+}$ ,  $\text{Na}^+$ ,  $\text{Mg}^{2+}$ ,  $\text{K}^+$ ) were analyzed using ion chromatography (Dionex ICS-90). This system was outfitted with a separation column (Dionex AS14A for anion and CS12A for cation), a guard column (Dionex AG14A for anion and CG12A for cation), and a conductivity detector (Dionex DS5).

---

**Characteristics and  
source  
apportionment of  
atmospheric aerosols**

---

H. Xu et al.

[Title Page](#)[Abstract](#)[Introduction](#)[Conclusions](#)[References](#)[Tables](#)[Figures](#)[⏪](#)[⏩](#)[◀](#)[▶](#)[Back](#)[Close](#)[Full Screen / Esc](#)[Printer-friendly Version](#)[Interactive Discussion](#)

A gradient weak base eluent ( $3.5 \text{ mmol L}^{-1} \text{ Na}_2\text{CO}_3$ ;  $1 \text{ mmol L}^{-1} \text{ NaHCO}_3$ ) was used for anion detection, while a weak acid eluent ( $22 \text{ mmol L}^{-1} \text{ MSA}$ ) was used for cation detection. Ion recovery was in the range of 80 to 120%. The relative standard deviation (SD) of each ion was less than 3% for the reproducibility test. Limits of detection (S/N=3) were less than  $0.03 \text{ mg L}^{-1}$  for anions and  $0.004 \text{ mg L}^{-1}$  for cations. Quality assurance was routinely carried out using standard reference materials (Merck Co.). Data from blank samples was subtracted from the corresponding sample data after analysis.

### 2.2.2 Element analysis

Half of each filter was treated with microwave digestion. Forty five minute extractions were performed into a mixture of 3 ml AR grade hydrochloric acid (37%) and 8 ml AR grade nitric acid (68%). A Multiwave3000 microwave digestion machine was used with the following conditions: power=1400 W; maximum temperature=180°; maximum pressure=22 atm.

Upon cooling, the solutions were diluted to 50 ml with deionized water ( $18 \text{ M}\Omega \text{ cm}^{-1}$  resistivity). Nineteen elements were characterized using an inductively coupled plasma mass spectrometer (ICP-MS, model, 7500a, Agilent Co., USA). Experimental conditions were: RF power=1350 W; carrier gas flow rate= $1.12 \text{ L min}^{-1}$ ; PeriPump=0.1 rps; S/C temp=2°; oxide: 156/140<0.45%; doubly charged: 70/140<1.01%. The concentrations of trace metal elements, including Ca, Fe, Al, Mg, Ba, Sr, Zr, K, Pb, Zn, As, Sn, Cd, Cu, Na, Cr, Mn, Ni, and V, were analyzed.

### 3 Results and discussion

#### 3.1 Concentration of water soluble ions and metal elements

Water-soluble ion concentrations of TSP at the summit of Mount Tai are shown in Table 1, which also shows concentrations of PM<sub>10</sub> and PM<sub>2.5</sub> at Mount Gongga, Mount Changbai, Mount Dinghu, Beijing, and Shanghai. Figure 2 indicates that water-soluble ion concentrations, especially secondary ions such as SO<sub>4</sub><sup>2-</sup>, NH<sub>4</sub><sup>+</sup>, and NO<sub>3</sub><sup>-</sup>, reside mainly within PM<sub>10</sub>, and K<sup>+</sup> concentrations reside mainly within PM<sub>2.5</sub>. Although particle sizes from these different sites were not uniform, the water-soluble ion concentrations can still be compared, especially for secondary ions (i.e., SO<sub>4</sub><sup>2-</sup>, NH<sub>4</sub><sup>+</sup>, NO<sub>3</sub><sup>-</sup> and K<sup>+</sup>). Water-soluble ion concentrations at the summit of Mount Tai were much higher than those at the atmospheric background station. Secondary ion concentrations at the summit of Mount Tai were 9 to 109 times higher than those of Waliguan baseline station, Mount Longfeng, and Lin'an regional background stations, and they were 4 to 17 times higher than those of Mount Gonggai, Mount Changbai, and Mount Dinghu forest ecosystem station. In contrast, secondary ion concentrations at the summit of Mount Tai were close to those in Beijing, Shanghai. Therefore, aerosol pollution at the summit of Mount Tai appears to be deeply affected by regional pollution in North China. It was found that the sulfate concentration of Mount Tai was 2.2 times lower than that obtained via aircraft measurement (January, 1994 North China). The emission of SO<sub>2</sub>, which is a sulfate precursor, has not decreased from 1994 to 2006 (Streets et al., 2000). Higher sulfate concentrations from aircraft measurements were mostly likely due to the sampling season, as the aircraft measurement was run in winter and this Mount Tai experiment was performed in summer. The large amount of coal combusted for heating during the North China winter emits SO<sub>2</sub>, which is mostly transformed into sulfate. A relatively small amount of SO<sub>2</sub>, however, is emitted in summertime. The nitrate concentration of Mount Tai is 2.6 times higher than that of the aircraft measurement. This is in accord with previous results, which report that nitrogen oxide, a precursor of ni-

## Characteristics and source apportionment of atmospheric aerosols

H. Xu et al.

Title Page

Abstract

Introduction

Conclusions

References

Tables

Figures

⏪

⏩

◀

▶

Back

Close

Full Screen / Esc

Printer-friendly Version

Interactive Discussion

trate, has increased in concentration every year (Andreas et al., 2005). Ammonium and metal ion concentrations are close to those of aircraft measurements. Elevation of the Mount Tai sample site was close to the average height of aircraft measurements. Therefore, the results of this Mount Tai experiment can be used to deduce the regional characteristics of North China.

Concentrations of the crustal elements Na, Mg, Al, Ca, and Fe were  $0.78$  to  $8.37 \mu\text{g m}^{-3}$ , or 96.2% of the total metallic element concentrations detected. Concentrations of the metallic elements Mn, Ni, Cu, Sb, Ba, Zn, and Pb were  $0.02$  to  $0.17 \mu\text{g m}^{-3}$ . Concentrations of metal elements Co, Mo, and Ti were less than  $0.01 \mu\text{g m}^{-3}$ . Results were compared with reported metallic element concentrations in aerosols of Chinese cities (Gao et al., 1996; Wei et al., 2001; Yang et al., 2002). We found that Mount Tai crustal element concentrations were somewhat higher than those of cities. Mount Tai metal element concentrations (e.g., Zn and Pb), which are mostly from anthropogenic pollution sources, were much lower than those of cities. Elements such as Zn and Pb mainly result from direct emission from pollution sources; however, water-soluble ions such as  $\text{SO}_4^{2-}$ ,  $\text{NO}_3^-$ , and  $\text{NH}_4^+$  are secondary pollutants, which come from the chemical transformation of  $\text{SO}_2$ ,  $\text{NO}_x$ , and  $\text{NH}_3$ , respectively. This indicates that secondary pollutants are easier than primary pollutants to transport via aerosols in regional areas.

### 3.2 Size distribution of water-soluble ions and metal elements

Typical size distributions obtained for trace metal elements and ions are illustrated in Fig. 2. Three size distributions were found for the water-soluble ions, including masses within: (1) the accumulation mode, with a peak at  $0.43$  to  $0.65 \mu\text{m}$  ( $\text{SO}_4^{2-}$ ,  $\text{NH}_4^+$ , and  $\text{K}^+$ ), (2) coarse particles, with a peak at  $4.7$  to  $5.8 \mu\text{m}$  ( $\text{Ca}^{2+}$  and  $\text{Mg}^{2+}$ ), (3) two modes, with peaks at  $0.43$  to  $0.65 \mu\text{m}$  and  $4.7$  to  $5.8 \mu\text{m}$  ( $\text{NO}_3^-$ ,  $\text{Na}^+$ , and  $\text{Cl}^-$ ). Three size distributions were also found for the trace metal elements, including masses within: (1) coarse particles, with a peak at  $4.7$  to  $5.8 \mu\text{m}$  (Mg, Al, Fe, Ca, Mn, and Ba), (2) the

## Characteristics and source apportionment of atmospheric aerosols

H. Xu et al.

Title Page

Abstract

Introduction

Conclusions

References

Tables

Figures

⏪

⏩

◀

▶

Back

Close

Full Screen / Esc

Printer-friendly Version

Interactive Discussion

accumulation mode, with a peak at 0.43 to 1.1  $\mu\text{m}$  (Pb, Zn, and Ti), (3) two modes, with peaks at 0.43 to 1.1  $\mu\text{m}$  and 4.7 to 5.8  $\mu\text{m}$  (Co, Ni, Mo, Na, and Cu).

$\text{SO}_4^{2-}$  was found in the accumulation mode, with 87% of its mass present as fine particles with aerodynamic diameters less than 2.1  $\mu\text{m}$ . During the observation period, sulfate size distributions exhibited little variation, and the median aerodynamic diameter (MMAD) remained within 0.2 to 0.8  $\mu\text{m}$ . Sulfate existed mainly in “accumulation mode” and “droplet mode” states. The MMAD increased with increasing sulfate concentration when it was less than 10  $\mu\text{g m}^{-3}$ ; however, when the sulfate concentration was larger than 10  $\mu\text{g m}^{-3}$ , the MMAD remained between 0.5 and 0.8  $\mu\text{m}$ , putting it in the “droplet mode”. This indicated that the high sulfate concentration was due to aqueous phase reactions in fog and cloud droplets or to hygroscopic growth of aerosols from the smaller accumulation mode. The sulfate size distributions were close to those from summer and fall in Beijing (Yao et al., 2003; Hu et al., 2005; Xu et al., 2007), further indicating that aerosol pollution at the summit of Mount Tai is affected by regional pollution in North China.

Metallic elements, such as Mg, Al, Fe, Ca, Mn, and Ba, were found in the coarse mode, with more than 80% of their mass present as coarse particles with aerodynamic diameters greater than 2.1  $\mu\text{m}$ . Mg, Al, Fe, and Ca are typical crustal elements; thus, these elements likely come from wind-blown soil. Metallic elements, such as Pb, Zn, and Ti, as well as the ions  $\text{SO}_4^{2-}$ ,  $\text{NH}_4^+$ , and  $\text{K}^+$ , were found in the accumulation mode, with more than 70% of their mass present as fine particles with aerodynamic diameters from 0.43  $\mu\text{m}$  to 2.1  $\mu\text{m}$ . Pb, Zn, and  $\text{K}^+$  are mainly a consequence of fossil fuel (e.g., coal, oil, and biomass) combustion.  $\text{SO}_4^{2-}$  and  $\text{NH}_4^+$  mainly result from the process of  $\text{SO}_2$  and  $\text{NH}_3$  secondary particle formation. These elements and ions have a small peak between 4.7 and 5.8  $\mu\text{m}$ . Thus, we conclude that the surface of coarse particles have sorptive interactions with them. Metallic elements, such as Co, Ni, Mo, Na, and Cu, have a peak between 4.7 and 5.8  $\mu\text{m}$ , but they distribute evenly among all modes. The sources of these elements are complex, as there are coarse particles from anthropogenic emissions (e.g., coal burning) and fine particles from natural

## Characteristics and source apportionment of atmospheric aerosols

H. Xu et al.

Title Page

Abstract

Introduction

Conclusions

References

Tables

Figures

⏪

⏩

◀

▶

Back

Close

Full Screen / Esc

Printer-friendly Version

Interactive Discussion



emissions (e.g., wind-blown dust).  $\text{NO}_3^-$  and  $\text{Cl}^-$  have obvious peaks between 0.65 and  $1.1\ \mu\text{m}$  as well as between 4.7 and  $5.8\ \mu\text{m}$ .  $\text{NO}_3^-$  mainly arises from secondary particles formed by  $\text{NO}_x$ . Nitrate is more easily dissolved in water than sulfate and is thus more easily absorbed to the surface of coarse particles, resulting in the high peak from 4.7 to  $5.8\ \mu\text{m}$ . Although  $\text{Cl}^-$  is bimodal, it distributes evenly among all diameters.  $\text{Cl}^-$  mainly comes from sea salt and is absorbed by particles of every diameter during long-distance movements and transformations, making the  $\text{Cl}^-$  size distribution smoother.

### 3.3 Temporal variation

Secondary ions and  $\text{K}^+$  had large variations in concentration, while others had relatively little variation, as shown in Fig. 3. At high concentrations of secondary ions and  $\text{K}^+$ , differences between day and night were obvious. For example, sulfate concentration during the daytime was four times higher than at nighttime for 11 through 12 June. Average concentrations of all ions (excluding  $\text{K}^+$ ) in the day were higher than those at night. This was especially true for sulfate, which had daytime concentrations 41% higher than those at night. Observation conditions included average wind speeds of  $5.4\ \text{m s}^{-1}$  and  $8.3\ \text{m s}^{-1}$  for day and night, respectively. It is important to note that ion concentrations (e.g., sulfate) were likely low at night due to faster average wind speeds, which can more easily diffuse pollutants. Aerosols emitted by biomass combustion contain high concentrations of  $\text{K}^+$  (Song et al., 2002; Sun et al., 2004; Xu et al., 2007). The  $\text{K}^+$  concentration at Mount Tai is affected by sources of biomass combustion nearby. Observed high concentrations of  $\text{K}^+$  at night were most likely due to the time of biomass combustion and transport in North China. For most metallic elements, the difference between measurements taking during the day and the night was also obvious, with higher average concentrations during the day. For example, Ni concentrations during the day were 1.6 times higher than those at night. This indicates that metallic element concentrations can be influenced by convection processes in the

**Characteristics and  
source  
apportionment of  
atmospheric aerosols**

H. Xu et al.

Title Page

Abstract

Introduction

Conclusions

References

Tables

Figures

⏪

⏩

◀

▶

Back

Close

Full Screen / Esc

Printer-friendly Version

Interactive Discussion

atmospheric boundary layer.

Air mass trajectories from 1 to 30 June were calculated to assess the importance of different source regions on aerosol composition at the sampling sites. The HYSPLIT 4 model from the Air Resources Laboratory of NOAA (<http://www.arl.noaa.gov/ready/hysplit4.html>) was used for this purpose. FNL meteorological data was used as the input. On each sampling day, two 24 h back trajectories were computed at 00:00 and 12:00. Statistical analysis of these calculated trajectory directions indicated that there were mainly two sectors with different air compositions. These were: (1) the south sector of Mount Tai, including the south area of Shandong province, Jiangsu province, and Anhui province, which belong to the Changjiang delta; (2) the north sector of Mount Tai, including the north area of Shandong province, Hebei province, the Inner Mongolia autonomy region, Beijing, and Tianjin, which surround the Bohai. Two representative trajectories are shown in Fig. 4. As in Fig. 3, sulfate had the greatest variety, with its lowest concentration at  $4.0 \mu\text{g m}^{-3}$  and its highest concentration at  $42.3 \mu\text{g m}^{-3}$ . The sulfate concentration reached its highest value from 5 to 6, 11 to 12 June, 19 to 23 June, and 28 to 29 June. During these four time periods, the sampling sites were mainly influenced by air from the south sector. For example, it had an increasing amount of sulfate from 1 to 7 June and then a decreasing amount from 8 to 10 June, when the sulfate concentration dropped to  $9.9 \mu\text{g m}^{-3}$  from its highest value ( $42.3 \mu\text{g m}^{-3}$ ). The wind direction and humidity were completely different during these two processes. The wind, with an average speed of  $5.0 \text{ m s}^{-1}$ , was always from the south and had a relative humidity of 69% from 1 to 7 June. Wind with an average speed of  $7.3 \text{ m s}^{-1}$  was mainly from the north and had a relative humidity of 45% from 8 to 10 June. This indicates that air from the south carries a lot of sulfate and is wet, which enables formation of high sulfate concentrations within the “droplet mode”. Furthermore, the city of Tai’an is located to the south of Mount Tai. This local Tai’an pollution is an important source for the formation of high sulfate concentrations. Metallic elements (e.g., Zn and Pb), which are produced mainly from anthropogenic pollution sources, reached high values of  $0.300 \mu\text{g m}^{-3}$  and  $0.171 \mu\text{g m}^{-3}$ , respectively, from 5

**Characteristics and source apportionment of atmospheric aerosols**

H. Xu et al.

Title Page

Abstract

Introduction

Conclusions

References

Tables

Figures

⏪

⏩

◀

▶

Back

Close

Full Screen / Esc

Printer-friendly Version

Interactive Discussion

to 6 June. Crustal elements, however, showed no obvious concentration increase during the same time period. Air from the south comes mainly from heavy polluted areas (e.g., Changjiang delta), and the wind speed is low, making it difficult for pollution to diffuse. For example, the average wind speed was  $2.6 \text{ m s}^{-1}$  on 5 June.

5 Sulfate concentration was low from 9 to 10 June, when the sampling sites were mainly influenced by air from the north sector. This indicates that air from the north carries little sulfate. During this period, crustal elements (e.g., Mg and Al) reached their highest concentrations at  $2.2 \mu\text{g m}^{-3}$  and  $5.1 \mu\text{g m}^{-3}$ , respectively. These values are 2.1 times higher than average. Metallic elements (e.g., Zn and Pb), however, exhibited  
10 no obvious concentration increase during the same period. This indicates that dry air from the north can easily raise dust from soil, thus causing the crustal element concentrations to increase.

Nitrate and ammoniate exhibited the same variations as sulfate, suggesting that these three types of ions have similar sources. Variations in nitrate and ammoniate  
15 concentrations were smaller than those of sulfate. One possible cause of this is that nitrate and ammoniate decompose more easily than sulfate, making it more difficult to reach high concentrations via accumulation.  $\text{K}^+$  had the same concentration variations as for secondary ions prior to 13 June; however, the  $\text{K}^+$  concentrations remained low and exhibited completely different variation characteristics after 13 June. A potential  
20 reason for this is that biomass combustion in North China occurs mainly during the first half of June. High  $\text{K}^+$  concentrations from biomass combustion are influenced by meteorological factors (e.g., wind direction and humidity), which is similar for secondary ions.  $\text{K}^+$  arising mainly from soil dust, however, had little variation after 13 June.

#### 4 Summary and conclusions

25 Water-soluble ion concentrations in aerosols at the summit of Mount Tai were much higher than those at the atmospheric background station, which indicates the regional characteristics of North China. Metallic elements in aerosols at the summit of Mount

---

## Characteristics and source apportionment of atmospheric aerosols

H. Xu et al.

---

Title Page

Abstract

Introduction

Conclusions

References

Tables

Figures

⏪

⏩

◀

▶

Back

Close

Full Screen / Esc

Printer-friendly Version

Interactive Discussion

Tai also exhibited regional pollution characteristics, offering data for research into the transport of pollution between eastern China and the Pacific.

The secondary ions  $\text{SO}_4^{2-}$ ,  $\text{NH}_4^+$ ,  $\text{NO}_3^-$ , and  $\text{K}^+$  mainly resided within fine particles. Secondary ions mainly come from long-term transport processes, while  $\text{K}^+$  arises mainly from biomass combustion in North China. Elements including Ca (including  $\text{Ca}^{2+}$ ), Mg (including  $\text{Mg}^{2+}$ ), Al, Fe, Mn, and Ba mainly resided within coarse particles, which come from soil dust. Elements including Zn and Pb mainly resided within fine particles, which come from industry emissions.

High sulfate concentrations were present mainly in “droplet mode” states. These can be attributed to aqueous phase reactions in fog and cloud droplets or to the hygroscopic growth of aerosols from the smaller accumulation mode.

Secondary ion and  $\text{K}^+$  concentrations exhibited large variation. Wind direction and humidity were key factors in this variation, along with the sources and sinks that influence variation. Dry air from the north led to an increase in crustal element (e.g., Mg and Al) concentrations, while air from the south led to an increase in pollution element (e.g., Zn and Pb) concentrations. This demonstrates the regional pollution characteristics of North China.

*Acknowledgements.* This work was supported by the National Natural Science Foundation of China under Grant No. 40525016; National Basic Research Program of China (973) under Grant No. 2007CB407303 and 2006CB403701; Hi-tech Research and Development Program of China(863) under Grant No. 2006AA06A301. Thanks are given to Professor Wang Zifa and Professor Hajime Akimoto for their organization of the observation project, and to the Mount Tai meteorological observation station.

## References

- Andreas, R., John, P. B., Hendrik, N., Claire, G., and Ulrike, N.: Increase in tropospheric nitrogen dioxide over China observed from space, *Nature*, 437, 129–132, 2005.
- Christoph, H., Robert, G., Urs, B., Martin, G., Christian, M., and Heinze, V.: Chemical characterization of  $\text{PM}_{2.5}$ ,  $\text{PM}_{10}$  and coarse particles at urban, near-city and rural sites in Switzerland, *Atmos. Environ.*, 39, 637–651, 2005.

## Characteristics and source apportionment of atmospheric aerosols

H. Xu et al.

Title Page

Abstract

Introduction

Conclusions

References

Tables

Figures

⏪

⏩

◀

▶

Back

Close

Full Screen / Esc

Printer-friendly Version

Interactive Discussion



- Englert, N.: Fine particles and human health- a review of epidemiological studies, *Toxicol. Lett.*, 149, 235–242, 2004.
- Gao, J., Wang, T., Ding, A. J., and Liu, C. B.: Observational study of ozone and carbon monoxide at the summit of Mount Tai (1534 m.a.s.l) in the central-eastern China, *Atmos. Environ.*, 39, 4779–4791, 2005.
- Gao, J. H., Wang, W., Du, J., Liu, H. J., Pang, Y. B., and Tang, D. G.: Preliminary study on the aerosol characteristics of Xiamen in spring, *Research of Environmental Sciences*, 9(5), 33–37, 1996 (in Chinese).
- Hu, M., Zhao, Y. L., He, L. Y., Huang, X. F., Tang, X. Y., Yao, X. H., and Chen, Z. Q.: Mass size distribution of Beijing particulate matters and its inorganic water-soluble ions in winter and summer, *Environ. Sci.*, 26(4), 1–6, 2005 (in Chinese).
- Seinfeld, J. H. and Pandis, S. N.: *Atmospheric Chemistry and Physics-from air pollution to climate change*, John Wiley & Sons, New York, 1998.
- Streets, D. G. and Waldhoff, S. T.: Present and future emissions of air pollutants in China: SO<sub>2</sub>, NO<sub>x</sub> and CO, *Atmos. Environ.*, 34, 363–374, 2000.
- Sun, Y. L., Zhuang, G. S., Wang, Y., Han, L. H., Guo, J. H., Dan, M., Zhang, W. J., Wang, Z. F., and Hao, Z. P.: The air-borne particulate pollution in Beijing -concentration, composition, distribution and sources, *Atmos. Environ.*, 38, 5991–6004, 2004.
- Song, Y., Tang, X. Y., Fang, C., Zhang, Y. H., Hu, M., and Ceng, L. M.: Source apportionment on fine particles in Beijing, *Environ. Sci.*, 23(6), 11–16, 2002 (in Chinese).
- Wang, W., Tang, D. G., Liu, H. J., Wang, M. Y., and Du, J.: Aircraft measurement of atmospheric pollutants in winter in North China II: research on pollution properties of atmospheric aerosol, *Research of Environmental Sciences*, 13(1), 10–13, 2000 (in Chinese).
- Wei, F. S., Teng, E. J., Wu, G. P., Hu, W., Wilson, W. E., Chapman, R. S., Pau, J. C., and Zhang, J.: Concentrations and elemental components of PM<sub>2.5</sub>, PM<sub>10</sub> in ambient air in four large Chinese cities, *Environment Monitoring in China*, 17(7), 1–6, 2001 (in Chinese).
- Xu, H. H., Wang, Y. S., Wen, T. X., and He, X. X.: Size distributions and vertical distributions of water soluble ions of atmospheric aerosol in Beijing, *Environ. Sci.*, 28(1), 14–19, 2007 (in Chinese).
- Yang, D. Z., Yu, X. L., Fang, X. M., Wu, F., and Li, X. S.: A study of aerosol at regional background stations and baseline station, *J. Appl. Meteorol.*, 7(4), 396–405, 1996 (in Chinese).
- Yang, D. Z., Yu, H. Q., Ding, G. A., Wang, S. F., and He, Z. S.: An analysis of aerosols in the lower-level atmosphere over Beijing northern suburbs in winter, *J. Appl. Meteorol.*,

---

## Characteristics and source apportionment of atmospheric aerosols

H. Xu et al.

---

Title Page

Abstract

Introduction

Conclusions

References

Tables

Figures

◀

▶

◀

▶

Back

Close

Full Screen / Esc

Printer-friendly Version

Interactive Discussion



13(Suppl.), 113–126, 2002 (in Chinese).

Yao, X. H., Chan, C. K., Fang, M., Cadle, S., Chan, T., Mulawa, P., He, K. B., and Ye, B. M.: The water-soluble ionic composition of PM<sub>2.5</sub> in Shanghai and Beijing, China, Atmos. Environ., 36, 4223–4234, 2002.

- 5 Yao, X. H., Lau, A. P. S., Fang, M., Chan, C. K., and Hu, M.: Size distributions and formation of ionic species in atmospheric particulate pollutants in Beijing, China: 1-inorganic ions, Atmos. Environ., 37, 2991–3000, 2003.

ACPD

9, 16361–16379, 2009

---

**Characteristics and  
source  
apportionment of  
atmospheric aerosols**

H. Xu et al.

---

Title Page

Abstract

Introduction

Conclusions

References

Tables

Figures

⏪

⏩

◀

▶

Back

Close

Full Screen / Esc

Printer-friendly Version

Interactive Discussion

**Table 1.** Average water-soluble ion concentrations for atmospheric aerosols in different locations ( $\mu\text{g m}^{-3}$ ).

Sample site	Sample time	$\text{SO}_4^{2-}$	$\text{NO}_3^-$	$\text{Cl}^-$	$\text{NH}_4^+$	$\text{Ca}^{2+}$	$\text{Na}^+$	$\text{Mg}^{2+}$	$\text{K}^+$
Waliguan(TSP) <sup>a</sup> , 3816 m	1994-10, 1995-01	0.20	0.12	0.28	0.29				
Mount Longfeng(TSP) <sup>a</sup> , 331 m		0.88	0.69	0.45	0.87				
Lin'an (TSP) <sup>a</sup> , 131 m		1.51	0.70	0.66	1.00				
Mount Gongga(PM <sub>10</sub> ), 3000 m	2006-06	4.42	0.79	0.23	1.47	0.07	0.13	0.45	0.21
Mount Changbai(PM <sub>10</sub> ), 2691 m	2006-06	2.79	0.52	0.34	1.11	0.09	0.04	0.02	0.12
Mount Dinghu(PM <sub>10</sub> ), 1000 m	2006-06	7.88	1.74	0.45	2.65	0.35	0.56	0.08	0.37
Aircraft measurement in North China(TSP) <sup>b</sup> , average 1500 m	1994-01	41.46	4.95	5.72	6.49	6.15	2.46	0.81	3.46
Shanghai(PM <sub>2.5</sub> ) <sup>c</sup>	1999-03, 2000-06	15.55	6.65	1.75	6.4	0.45	0.65	0.30	1.95
Beijing(PM <sub>2.5</sub> ) <sup>c</sup>		17.65	10.10	1.70	6.35	0.75	0.70	0.35	2.20
Beijing(PM <sub>10</sub> ) <sup>d</sup>	2002-06, 2002-07	25.03	19.30	2.63	11.6				1.73
Mount Tai(TSP), 1534m	2006-06	20.05	13.72	3.13	9.72	6.67	1.08	0.33	3.21

<sup>a</sup> Yang Dongzhen et al., 1996.

<sup>b</sup> Wang Wei et al., 2000.

<sup>c</sup> Yao et al., 2002.

<sup>d</sup> Sun et al., 2004.

## Characteristics and source apportionment of atmospheric aerosols

H. Xu et al.

Title Page

Abstract

Introduction

Conclusions

References

Tables

Figures

◀

▶

◀

▶

Back

Close

Full Screen / Esc

Printer-friendly Version

Interactive Discussion

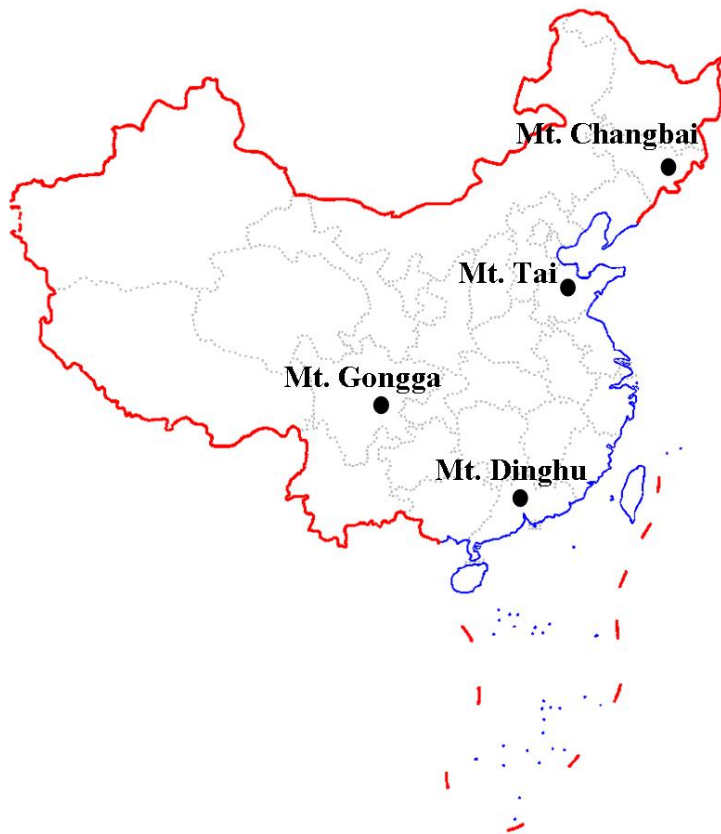


**Fig. 1.** Location of the observation site, including Mt. Tai ( $36^{\circ}16' N$ ,  $117^{\circ}06' E$ , 1534 m a.s.l.), Mt. Gongga ( $29^{\circ}35' N$ ,  $102^{\circ}00' E$ , 3000 m a.s.l.), Mt. Changbai ( $42^{\circ}24' N$ ,  $128^{\circ}28' E$ , 2691 m a.s.l.) and Mt. Dinghu ( $23^{\circ}10' N$ ,  $112^{\circ}32' E$ , 1000 m a.s.l.).

Characteristics and  
source  
apportionment of  
atmospheric aerosols

H. Xu et al.

Title Page

Abstract

Introduction

Conclusions

References

Tables

Figures

◀

▶

◀

▶

Back

Close

Full Screen / Esc

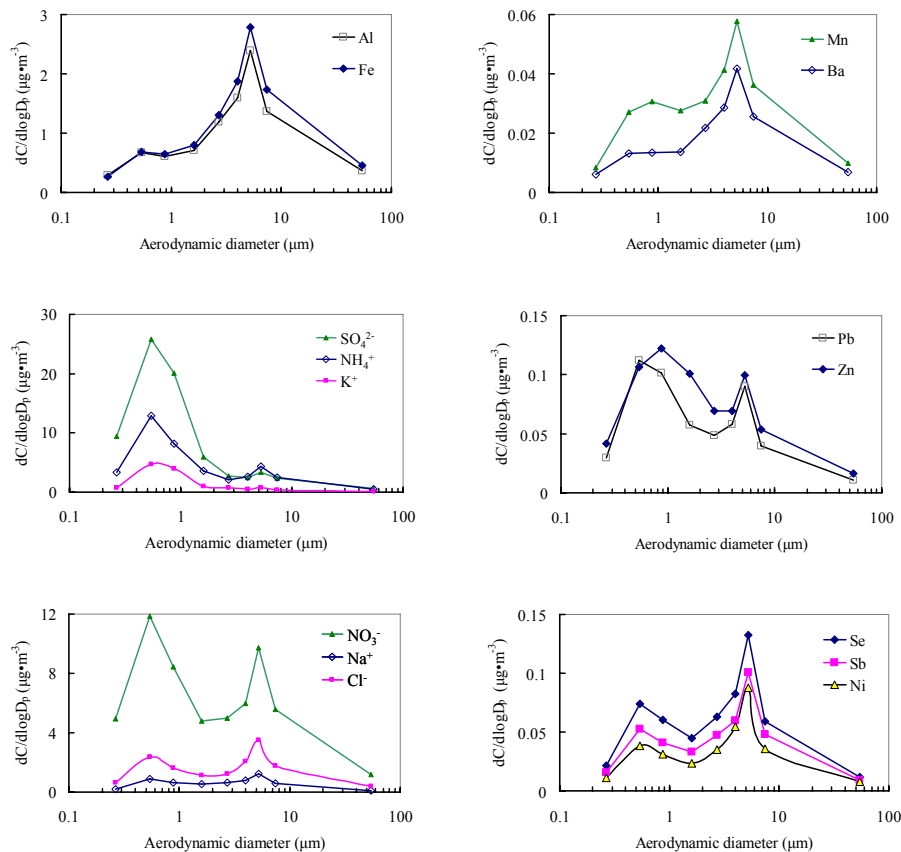
Printer-friendly Version

Interactive Discussion



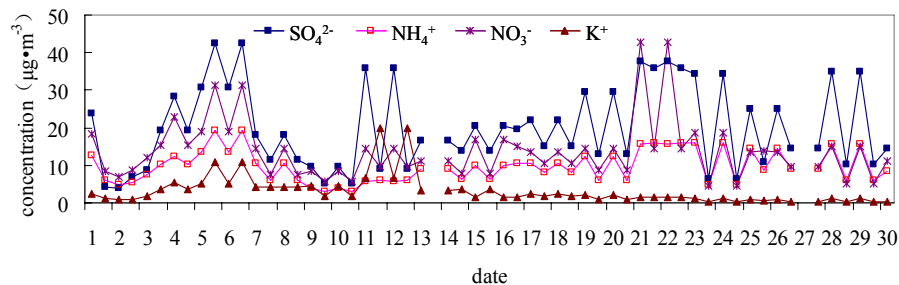
**Characteristics and source apportionment of atmospheric aerosols**

H. Xu et al.

**Fig. 2.** Typical size distributions of water-soluble ions and metal elements.[Title Page](#)[Abstract](#)[Introduction](#)[Conclusions](#)[References](#)[Tables](#)[Figures](#)[◀](#)[▶](#)[◀](#)[▶](#)[Back](#)[Close](#)[Full Screen / Esc](#)[Printer-friendly Version](#)[Interactive Discussion](#)

**Characteristics and  
source  
apportionment of  
atmospheric aerosols**

H. Xu et al.

**Fig. 3.** Variety of water-soluble ion concentrations.[Title Page](#)[Abstract](#)[Introduction](#)[Conclusions](#)[References](#)[Tables](#)[Figures](#)[◀](#)[▶](#)[◀](#)[▶](#)[Back](#)[Close](#)[Full Screen / Esc](#)[Printer-friendly Version](#)[Interactive Discussion](#)

**Characteristics and  
source  
apportionment of  
atmospheric aerosols**

H. Xu et al.

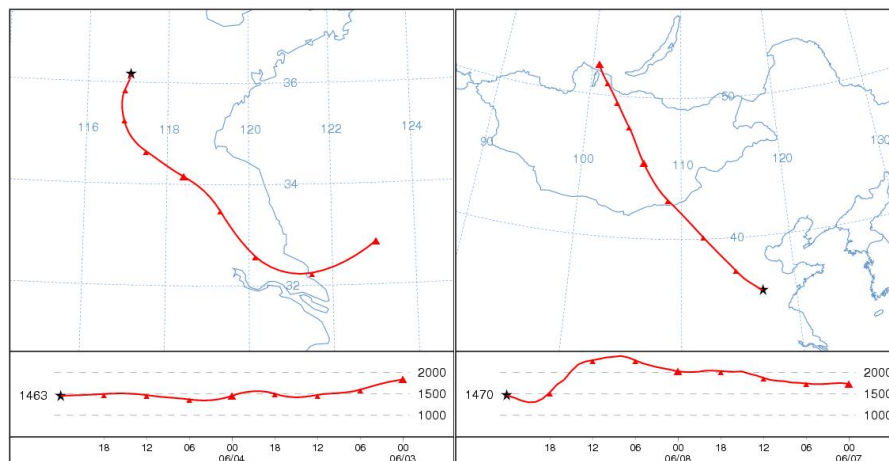


**Fig. 4.** Air mass arriving at Mount Tai at 00:00 on 5 June, 2006 as classified by backward trajectories (left); Air mass arriving at Mount Tai at 00:00 on 9 June, 2006 as classified by backward trajectories (right).

[Title Page](#)[Abstract](#)[Introduction](#)[Conclusions](#)[References](#)[Tables](#)[Figures](#)[⏪](#)[⏩](#)[◀](#)[▶](#)[Back](#)[Close](#)[Full Screen / Esc](#)[Printer-friendly Version](#)[Interactive Discussion](#)